

Resistivity scaling in metallic thin films and nanowires due to grain boundary and surface roughness scattering

Kristof Moors,^{1,2,*} Bart Sorée,^{2,3,4} and Wim Magnus^{2,3}

¹*KU Leuven, Institute for Theoretical Physics,
Celestijnenlaan 200D, B-3001 Leuven, Belgium*

²*Imec, Kapeldreef 75, B-3001 Leuven, Belgium*

³*University of Antwerp, Physics Department,
Groenenborgerlaan 171, B-2020 Antwerpen, Belgium*

⁴*KU Leuven, Electrical Engineering (ESAT) Department,
Kasteelpark Arenberg 10, B-3001 Leuven, Belgium*

(Dated: October 16, 2018)

Abstract

A modeling approach, based on an analytical solution of the semiclassical multi-subband Boltzmann transport equation, is presented to study resistivity scaling in metallic thin films and nanowires due to grain boundary and surface roughness scattering. While taking into account the detailed statistical properties of grains, roughness and barrier material as well as the metallic band structure and quantum mechanical aspects of scattering and confinement, the model does not rely on phenomenological fitting parameters.

* E-mail me at: kristof@itf.fys.kuleuven.be

I. INTRODUCTION

The resistivity of metallic thin films and nanowires increases drastically when the film thickness or wire diameter is reduced [1]. An increased resistivity is undesirable for typical applications of these structures, e.g. interconnects in semiconductor devices, as it leads to increased heating, power dissipation, signal propagation delays, et cetera. Hence, in order to assess the performance of metallic thin films and nanowires as conductors in nanoscaled applications, it is important to study their resistivity and scaling behavior and understand how a drastic increase of resistivity can be prevented, if at all possible for metallic structures with sub-10 nm dimensions.

Experimental data has indicated that the increase of resistivity is mainly induced by an increase of electron scattering at the grain boundaries and near the rough boundaries of the structure. These scattering mechanisms lead to a resistivity contribution that adds to the bulk resistivity dominated by the electron-phonon interaction and scattering with lattice imperfections which is, to a good approximation, independent of the thickness. The resistivity data of metallic thin films and wires is in good agreement with the semiclassical Mayadas-Shatzkes model, commonly used for data comparison and predicting a resistivity scaling almost inversely proportional to the film width or wire diameter [1, 2]. While the Mayadas-Shatzkes model provides satisfactory fits to the data, it contains phenomenological fitting parameters: a specularly parameter for boundary surface scattering and a reflection coefficient for grain boundary scattering. These parameters do not provide a clear connection between the microscopic scattering events and the resulting, measured resistivity of the thin film or nanowire. For example, there is no clear relation between boundary roughness, the microscopic origin of diffusive scattering at the boundary, and the phenomenological specularly parameter in the Mayadas-Shatzkes model which intends to capture this process. Moreover, the Mayadas-Shatzkes model neglects the material band structure properties and quantum mechanical aspects of scattering and confinement while a priori there is no reason to expect that both aspects have negligible impact on the resistivity scaling behavior.

We present an alternative approach to model resistivity scaling in metallic thin films and nanowires, based on the multi-subband Boltzmann transport equation, with averaged scattering rates obtained from Fermi's golden rule for grain boundary and surface roughness scattering [3, 4]. Our approach allows to perform a rigorous analysis of the resistivity and

its scaling behavior while taking into account the aforementioned aspects that are neglected in some conventional approaches.

In section II we summarize briefly the theory of the semiclassical multi-subband Boltzmann equation and the scattering rates obtained with Fermi's golden rule for grain boundary and surface roughness scattering. Next, we present some simulation results in section III, which are discussed in section IV, followed by a conclusion in section V. We also refer to some articles with similar developments for metallic thin films and nanowires [5–7].

II. THEORY

The electron (or hole) transport formalism based on the semiclassical multi-subband Boltzmann transport equation can be summarized by the following list of equations:

$$\mathbf{J} = \sum_{\mathbf{n}} \int \frac{d^D k}{(2\pi)^D} \frac{q \nabla_{\mathbf{k}} E_{\mathbf{n}}(\mathbf{k})}{\hbar} \delta f_{\mathbf{n}}(\mathbf{k}), \quad (1)$$

$$\delta f_{\mathbf{n}}(\mathbf{k}) = \frac{q \mathbf{E} \cdot \nabla_{\mathbf{k}} E_{\mathbf{n}}(\mathbf{k})}{\hbar} \tau_{\mathbf{n}}(\mathbf{k}) \delta(E_{\mathbf{n}}(\mathbf{k}) - E_{\text{F}}), \quad (2)$$

$$\frac{1}{\tau_{\mathbf{n}}(\mathbf{k})} = \sum_{\mathbf{n}', \mathbf{k}'} \left(1 - \frac{\tau_{\mathbf{n}'}(\mathbf{k}') \partial_{k'} E_{\mathbf{n}'}(\mathbf{k}')}{\tau_{\mathbf{n}}(\mathbf{k}) \partial_k E_{\mathbf{n}}(\mathbf{k})} \right) P(|\mathbf{n} \mathbf{k}\rangle \rightarrow |\mathbf{n}' \mathbf{k}'\rangle), \quad (3)$$

$$P(|i\rangle \rightarrow |f\rangle) = \frac{2\pi}{\hbar} |\langle i | V | f \rangle|^2 \delta(E_i - E_f), \quad (4)$$

where $\delta f_{\mathbf{n}}$ is the deviation of the distribution function from Fermi-Dirac equilibrium ($\delta f_{\mathbf{n}}(k) \equiv f_{\mathbf{n}}(\mathbf{k}) - f_{\mathbf{n}}^{\text{FD}}(\mathbf{k})$) for the (sub)band labeled by \mathbf{n} , $E_{\mathbf{n}}(\mathbf{k})$ and $\tau_{\mathbf{n}}(\mathbf{k})$ are respectively the energy and relaxation time for a state with wavevector \mathbf{k} (and k the component along the direction of the electric field) in (sub)band \mathbf{n} , q is the electron charge, \mathbf{E} the electric field, E_{F} the Fermi energy, V the scattering potential and \mathbf{J} the current density. The dimensionality of \mathbf{n} and \mathbf{k} depends on the system under consideration. The wavevectors \mathbf{k} are one-dimensional ($D = 1$) for nanowires and two-dimensional ($D = 2$) for thin films, while \mathbf{n} is a two-dimensional subband index vector for two-dimensional nanowire confinement and one-dimensional for thin film confinement (including an extra band index in both cases if required). The list of equations follows from the solution of the linearized Boltzmann equation at zero temperature [8]. The linearization and zero temperature assumption are justified in the case of small electric fields, elastic scattering and low enough temperatures ($k_{\text{B}}T \ll E_{\text{F}}$, with E_{F} measured from the lowest conduction band) and these are very reasonable assumptions for typical metallic nanowires and thin films at room temperature with

electrons predominantly subjected to grain boundary and surface roughness scattering. All the states $|\mathbf{n}^{(l)} \mathbf{k}^{(l)}\rangle$ that are considered in Eq. 1-4 are therefore Fermi level states with $E_{\mathbf{n}}(k) = E_{\mathbf{n}'}(k') = E_{\text{F}}$.

The relaxation times in Eq. 2 are coupled self-consistently through a system of linear equations and can be obtained through a matrix (of finite size for a nanowire while requiring numerical discretization of \mathbf{k} for thin films) inversion. Fermi's golden rule is invoked to obtain the scattering rates between the different electron states due to grain boundary and boundary surface roughness scattering. These scattering rates are averaged over an ensemble of grain boundaries and surface roughness profiles to retrieve a general and analytical expression which can be inserted into Eq. 3, allowing for fast and accurate simulations. Because electron-phonon and imperfection (e.g. point defects or impurities) scattering in thin films and nanowires do not deviate much from their bulk scattering behavior while being isotropic and independent from grain boundary and surface roughness scattering (Matthiessen's rule), their resistivity contribution is very close to the bulk value, ρ^{bulk} , and can be separated from the scaling part due to grain boundaries and surface roughness, ρ^{scaling} . This consideration leads to a total resistivity $\rho^{\text{bulk}} + \rho^{\text{scaling}}$, with ρ^{bulk} the bulk resistivity extracted from experiments and ρ^{scaling} resulting from the solution of Eqs. 1-4.

The input which is required to solve Eqs. 1-4 consists of a correct band structure profile of the nanowire or thin film, to be used in Eqs. 1-3, the wave functions of the electron states close to the Fermi level and expressions for the grain boundary and surface roughness potentials, entering the matrix elements in Eq. 4. The set of equations has no remaining free fitting parameters and the resistivity can be obtained without numerical integration.

For grain boundaries, we have borrowed the scattering potential and its distribution from the Mayadas-Shatzkes model [2]:

$$V^{\text{GB}}(x, y, z) = \sum_{\alpha=1}^N S^{\text{GB}} \delta(z - z_{\alpha}), \quad (5)$$

$$g(z_1, \dots, z_N) = \frac{\exp\left[-\sum_{\alpha} (z_{\alpha+1} - z_{\alpha} - D^{\text{GB}})^2 / 2(\sigma^{\text{GB}})^2\right]}{L_z [2\pi(\sigma^{\text{GB}})^2]^{(N-1)/2}}, \quad (6)$$

where the grain boundaries are represented by N Dirac delta barrier planes normal to the transport (z) direction at positions z_{α} , the barrier strength S^{GB} being distributed along the wire with an average distance D^{GB} in between subsequent grain boundaries and standard

deviation σ^{GB} . The average distance and standard deviation can be estimated from the experimental grain distribution while the barrier strength (having units of energy times length), representing the height and width of the grain boundary potential barrier, can be extracted from *ab initio* simulations. It typically depends on the orientation of the grains and their boundaries, but gives values of the order of magnitude of eV·Å. The normal orientation of the grain boundary planes in the Mayadas-Shatzkes model can be extended to random orientations but the deviations in resistivity from the results of grain boundaries with normal orientation are quite small [9].

For surface roughness, we consider the following potential and statistics, based on Ando's surface roughness scattering model [10]:

$$V^{\text{SR}}(\mathbf{r}) = U(x - \Delta(\mathbf{R}), y, z) - U(\mathbf{r}), \quad (7)$$

$$\langle \Delta(\mathbf{R}) \rangle = 0, \quad \langle \Delta(\mathbf{R})\Delta(\mathbf{R}') \rangle = \Delta^2 e^{-(\mathbf{R}-\mathbf{R}')^2/(\Lambda^2/2)}, \quad (8)$$

where $\mathbf{r} \equiv (x, y, z)$ and we assume a roughness function $\Delta(\mathbf{R})$ with $\mathbf{R} \equiv (y, z)$ that shifts the potential $U(\mathbf{r})$ along a confinement (x) direction as a function of the boundary position \mathbf{R} with zero average, standard deviation (or RMS) Δ and correlation length Λ . The matrix element is linear in V but not linear in Δ . One often expands the matrix element linearly in the roughness function in combination with considering an infinite potential well for $U(\mathbf{r})$, leading to the so called Prange-Nee approximation for surface roughness scattering [11]. This approximation neglects the oscillatory behavior of the wave functions and can lead to large errors on the scattering rates. We have recently introduced an analytical expression for the matrix elements going beyond the linear expansion restriction as well as the infinite potential well limit, hence avoiding additional approximations such as the commonly used Prange-Nee approximation [4]. In this way, the potential barrier outside the wire or film can also be adjusted to represent the surrounding barrier material accurately, improving once again the accuracy of the simulations. While the roughness RMS and correlation length can both be measured experimentally, the correlation length is often neglected as it requires high resolution surface imaging. A finite and accurate value of the correlation length could be very important for nanowires however, as it can facilitate the search for new types of state protection from backscattering that may improve the resistivity.

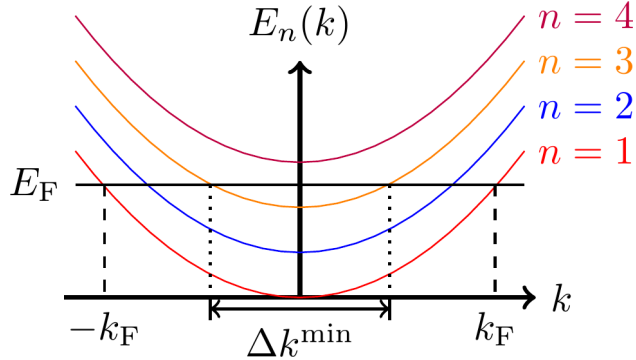


FIG. 1. A toy model band structure as a function of wave number k along the transport direction corresponding to an effective mass description of the electrons with (sub)bands labeled by integer n . The Fermi (maximal) wave number k_F is indicated as well as the minimal difference between positive and negative wave numbers Δk^{\min} at the Fermi energy level E_F .

III. RESULTS

We will present the scattering properties, based on the scattering potentials and statistics of Eq. 5-8, in the first subsection and the corresponding resistivity results for thin films and nanowires in the following subsection. For the sake of simplicity, the results are limited to thin films and nanowires represented by a finite potential well confining the electrons that are described in the effective mass approximation (see Fig. 1), although the present approach is generally applicable. The effective mass m_e^* and conduction electron density n_e are chosen to those of Cu: $m_e^* \approx m_e$, $n_e \approx 8.469 \times 10^{28} \text{ m}^{-3}$, $a_{\text{Cu}} \approx 0.361 \text{ nm}$.

A. Scattering

In Fig. 2 we show the scattering rates between pairs of initial (i) and final (f) states for grain boundary and surface roughness scattering. The two scattering mechanisms show very different behavior, the highest grain boundary and surface roughness scattering rates being concentrated along the anti-diagonal and diagonal in the (k_i, k_f) -plane respectively. We have included some additional averaging over random orientation of the grain boundary planes to obtain more realistic grain boundary scattering rates. This leads to deviations from perfect anti-diagonal coupling (corresponding to k to $-k$ backscattering) which follows

from the standard Mayadas-Shatzkes expression [9].

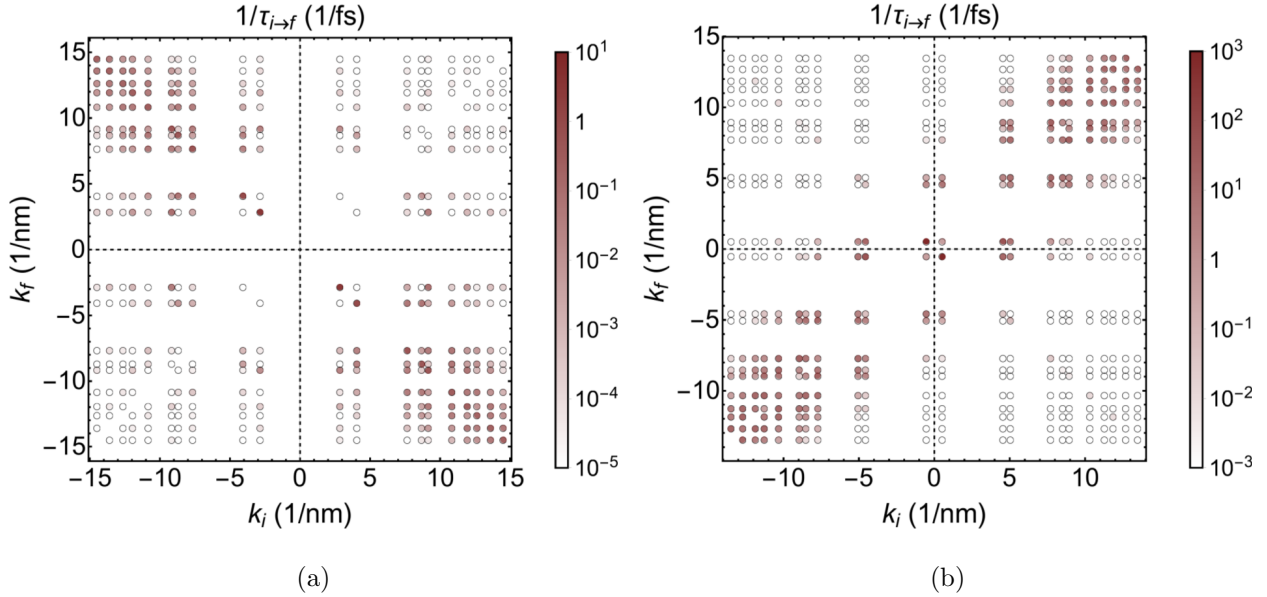


FIG. 2. The scattering rates between specific initial and final states are shown as a function of the wave number of the initial (k_i) and final (k_f) states for (a) grain boundary scattering (b) surface roughness scattering. A toy model system, with a limited number of subbands (or Fermi level states), is considered here for clarity, showing the important qualitative features.

B. Resistivity

The resistivity for thin films is presented in Fig. 3 as a function of the potential well barrier height and film thickness. In general, the resistivity increases with increasing barrier height or roughness RMS, and with decreasing roughness correlation length or film thickness. A maximal barrier height is obtained for a vacuum barrier and can be extracted from the work function W .

Fig. 4 exhibits the resistivity of nanowires as a function of their side lengths and for various grain boundary or surface roughness properties. We consider a square cross section for the nanowires and refer to the side length as the diameter. For grain boundaries we consider a linear relation between the diameter and the average inter-grain boundary distance as well as a sublinear relation. The result are very similar to those of thin films with the resistivity scaling purely determined by the inter-grain boundary distance and no visible additional effects of confinement. The standard deviation σ^{GB} is not studied, because as long as it

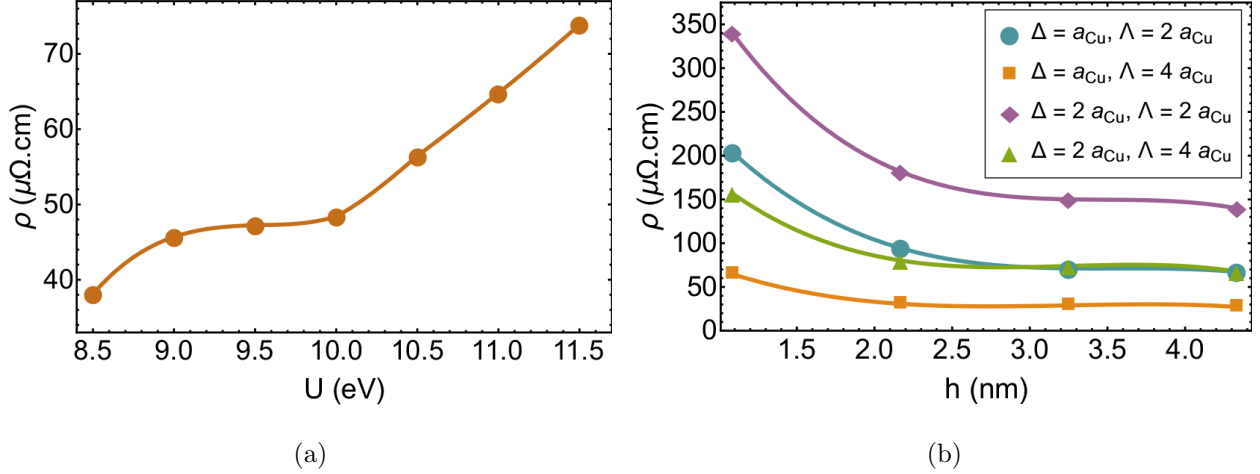


FIG. 3. The resistivity for rough metallic thin films is shown as a function of (a) the barrier potential height U for a film with thickness $h = 12 a_{\text{Cu}}$, roughness RMS $\Delta = a_{\text{Cu}}$ and correlation length $\Lambda = 2 a_{\text{Cu}}$ (b) the film thickness h with different surface roughness RMS and correlation length values. The vacuum potential barrier height is taken to be $U = 11.5$ eV.

is not substantially smaller than D^{GB} , resembling an unlikely periodic grain superlattice structure, its impact on the resistivity is negligible.

Surface roughness is studied for two cases, with different values for both the standard deviation and correlation length. A general trend of increasing resistivity for smaller diameters is observed, but there is no clear scaling exponent and large resistivity drops appear for certain diameters in case of sufficiently large roughness correlation lengths. These drops correspond to nanowires with a large minimum of the wave number difference Δk^{min} between Fermi level states with positive wave numbers and their negative counterparts (see Fig. 1).

IV. DISCUSSION

We have extracted useful information from the scattering rates of grain boundary and surface roughness scattering presented in Fig. 2 and the simulation results for resistivity scaling of thin films (Fig. 3) and nanowires (Fig. 4). Grain boundaries mostly induce backscattering which is barely affected by increasing confinement that accompanies shrinking side lengths. Hence, the resistivity scaling behavior is similar for thin films and nanowires and depends on the grain boundary strength and density. The average grain size and corresponding inter-grain boundary distance are equally crucial for thin films and nanowires and should

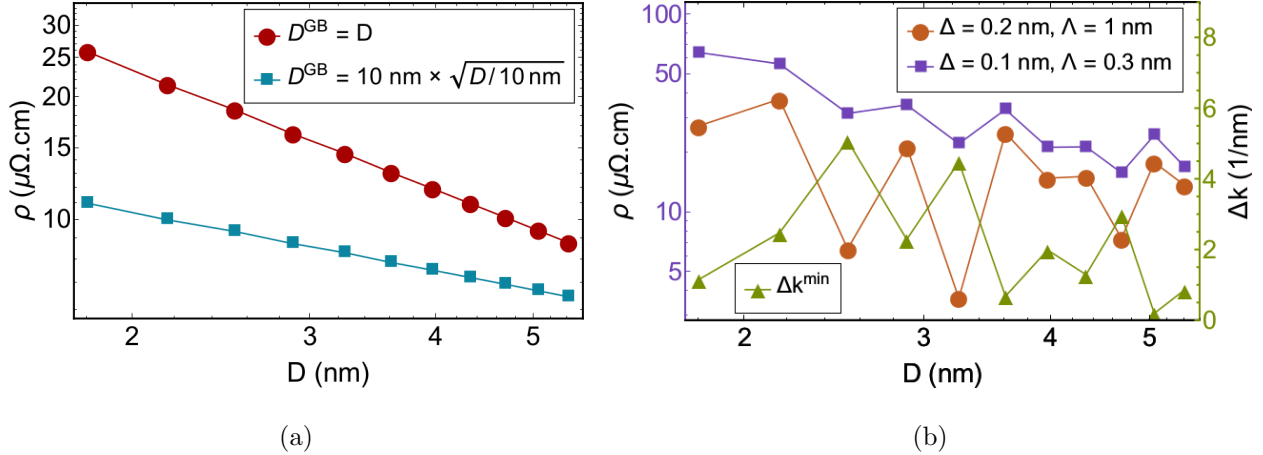


FIG. 4. The resistivity for metallic nanowires with (a) grain boundaries (b) boundary surface roughness is shown as a function of the nanowire diameter D . (a) Two different relations between the wire sides and the average inter-grain boundary distance are considered: linear and sublinear, with grain boundary strength $U^{\text{GB}} = a_{\text{Cu}} \times 1.5 \text{ eV}$. (b) Two different roughness profiles are shown, together with the minimal wave number difference Δk^{min} between Fermi level states with positive and negative wave numbers for each simulated diameter. A finite potential well with barrier height $U = E_{\text{F}} + W \approx 11.5 \text{ eV}$ is considered to represent vacuum.

be maximized for an optimal resistivity. It should be noted that the above results are obtained within the effective mass approximation. Consequently, when a more realistic band structure is adopted, together with more realistic grain boundary potentials, the scattering probability rates may be altered. But as the grains and their boundaries are typically randomly distributed and oriented throughout the structure, a significant suppression of grain boundary backscattering is generally not expected.

Boundary surface roughness causes very different scattering behavior as it mostly leads to scattering events with small scattering angles. While the corresponding scattering rates can be very large, there is no substantial loss of current as the transport velocity of the electrons is barely affected. Loss of current occurs largely through scattering events between states that have a wave number close to $k = 0$. This gives rise to typical resistivity scaling behavior for thin films, its resistivity value depending on the barrier height and specific roughness RMS and correlation length values, where we observe a non-quadratic relation between resistivity and barrier height due to the non-linear treatment of the surface roughness function. For nanowires however, drops in resistivity appear for certain diameters.

These drops coincide with the absence of Fermi level states close to $k = 0$. One can quantify this absence by looking at the minimal wave number difference Δk^{\min} between Fermi level states with positive k and those with negative k . A critical difference, $\Delta k^{\text{crit}} = \sqrt{8}/\Lambda$, can be retrieved from the roughness scattering matrix elements revealing that backscattering is suppressed exponentially when $\Delta k^{\min} > \Delta k^{\text{crit}}$, leading to a resistivity drop [4]. This drop cannot be explained merely in terms of a phenomenological specularly parameter and requires a scattering description with quantized transport wave vectors due to confinement and boundary surface roughness with a finite correlation length.

V. CONCLUSION

The resistivity scales up drastically when the diameter or thickness of nanowires and thin films drops below 100 nm. In the sub-10 nm regime, quantum mechanical effects of confinement and scattering come into play, introducing additional complexity for the resistivity scaling behavior. The simulation results show a general trend of increasing resistivity when the nanowire side lengths are reduced, but the typical resistivity scaling that is observed for larger wires and thin films is not pursued, mainly due to confinement changing the surface roughness scattering properties.

The transport model used to obtain the above mentioned results is based on the semi-classical multi-subband Boltzmann transport equation, while allowing for fast and accurate simulations without fitting parameters. These simulations in turn provide the means to perform a rigorous analysis of the impact of band structure and barrier properties as well as grain and roughness statistics on the resistivity scaling of metallic thin films or nanowires.

REFERENCES

-
- [1] D. Josell, S. H. Brongersma, Z. Tókei, Size-dependent resistivity in nanoscale interconnects, *Annual Review of Materials Research* 39 (2009) 231–254.
 - [2] A. Mayadas, M. Shatzkes, Electrical-resistivity model for polycrystalline films: the case of arbitrary reflection at external surfaces, *Physical Review B* 1 (4) (1970) 1382.

- [3] K. Moors, B. Sorée, Z. Tókei, W. Magnus, Resistivity scaling and electron relaxation times in metallic nanowires, *Journal of Applied Physics* 116 (6) (2014) 063714.
- [4] K. Moors, B. Sorée, W. Magnus, Modeling surface roughness scattering in metallic nanowires, *Journal of Applied Physics* 118 (12) (2015) 124307.
- [5] G. Fishman, D. Calecki, Surface-induced resistivity of ultrathin metallic films: a limit law, *Physical review letters* 62 (11) (1989) 1302.
- [6] G. Fishman, D. Calecki, Influence of surface roughness on the conductivity of metallic and semiconducting quasi-two-dimensional structures, *Physical Review B* 43 (14) (1991) 11581.
- [7] J. Feilhauer, M. Moško, Quantum and Boltzmann transport in a quasi-one-dimensional wire with rough edges, *Physical Review B* 83 (24) (2011) 245328.
- [8] C. Jacoboni, *Theory of Electron Transport in Semiconductors: A Pathway from Elementary Physics to Nonequilibrium Green Functions*, Vol. 165, Springer Science & Business Media, 2010.
- [9] K. Moors, B. Sorée, Z. Tókei, W. Magnus, Electron relaxation times and resistivity in metallic nanowires due to tilted grain boundary planes, in: *Ultimate Integration on Silicon (EUROSOU-ULIS)*, 2015 Joint International EUROSOU Workshop and International Conference on, IEEE, 2015, pp. 201–204.
- [10] T. Ando, A. B. Fowler, F. Stern, Electronic properties of two-dimensional systems, *Reviews of Modern Physics* 54 (2) (1982) 437.
- [11] R. Prange, T.-W. Nee, Quantum spectroscopy of the low-field oscillations in the surface impedance, *Physical Review* 168 (3) (1968) 779.